Potential Energy Surfaces for F−H_2 and Cl−H_2: Long-Range Interactions and Nonadiabatic Couplings†

Vincenzo Aquilanti, Simonetta Cavalli, Fernando Pirani, and Alessandro Volpi

Dipartimento di Chimica and INFM, Università di Perugia, 06123 Perugia, Italy

David Cappelletti*

Dipartimento di Ingegneria Civile ed Ambientale and INFM, Università di Perugia, 06125 Perugia, Italy

Received: October 16, 2000; In Final Form: January 3, 2001

The intermediate and long-range behavior of the three lowest doublet potential energy surfaces for the F(^2P_j)-H_2 and Cl(^2P_j)-H_2 systems has been studied, using a harmonic expansion of the potential, where the dependence on the relative orientation of the half-filled orbital of the open-shell atom and the molecular axis has been given in terms of bipolar spherical harmonics, whereas the coefficients modulate the effect of the variation of the intermolecular distance. The contribution of van der Waals, electrostatic, and charge-transfer interactions to the strength and the intermolecular distance dependence of each radial term are derived from previous molecular beam scattering experiments and from correlation formulas. The latter provide the link of these quantities to basic properties of the interacting partners. Besides describing elastic and inelastic channels, these surfaces also provide accurate information on the entrance channel for reactions.

I. Introduction

Chemical reactions and many inelastic processes typically involve open-shell species, which play a crucial role in the chemistry of atmospheres, plasmas, and lasers;[1] their interactions are described by a manifold of potential energy surfaces, among which nonadiabatic transitions occur and spin−orbit coupling may be operative. This is also of increasing modern relevance in view of the interest of ultracold collisions for astrophysical and Bose−Einstein condensation studies.[2]

Typical open-shell species can be atoms, free radicals, molecules such as NO, or atomic and molecular ions. Their interactions with closed shell molecules are weak (of the order of magnitude of 1 kcal/mol) and manifest from large (tens of Å) down to intermediate (a few Å) intermolecular distances. In this range, both the attractive interaction (due to dispersion, induction and charge transfer contributions) and the tail of the repulsion (determined by the size of the two partners) are operative. Electrostatic effects arise when permanent multipoles are present on both interacting partners; they often vanish when averaged over the spatial orientations of particles, but crucially affect the anisotropic part of the interaction.

Because of the small overlap of the electronic clouds, such interactions are unable to induce an appreciable modification in the internal structure of the involved species but can strongly affect the collision dynamics at thermal energies ($\leq$10 kcal/mol), defining the nature of steric effects which control the selectivity of chemical and physical elementary phenomena and determining transport and energy transfer processes which occur in various environments. These interactions depend on the relative orientation of the two partners, on the intermolecular distance and on coordinates defining the internal structure of the system: they are elusive to quantum chemistry and are known to an accuracy level often insufficient to adequately assess their influence on collision dynamics.

In this work, we consider the interactions of F(^2P_j) and Cl(^2P_j) atoms with the H_2 molecule, which are prototypes of open-shell atom−homonuclear diatomic molecule cases. These systems have been the object of many experimental (reaction rate constants,[3−5] elastic, inelastic, and reactive cross sections[6−18] and photoelectronic spectroscopy measurements[19−23]) and theoretical studies (ab initio potential energy surfaces[24−34] and reaction dynamics).[14,35−44]

Despite this long (and admittedly partial) list of references, the available results on the interaction from ab initio, semiempirical and empirical methods, are still unable to simultaneously reproduce all the existing experimental data. Three potential energy surfaces, two of A′ and one of A″ symmetry, must be considered to describe the evolution of the chemical reaction or of the energy exchange in the case of inelastic collisions. Theoretical information is especially precious for the description of the features of the ground potential energy surface in the neighborhood of the reaction transition state: this region mostly affects reactive scattering. The role of excited surfaces has been often neglected, and the intermediate and long-range behavior of the potential energy is known to a level of accuracy insufficient to satisfactorily account for experimental data such as elastic[8,10] and inelastic cross sections.[11,15,17] The most recent ab initio potential energy surface for F + H_2[32] appears to accurately reproduce many details of the reaction dynamics but a realistic entrance valley with possible refinements of the strong interaction region is required by new experiments.[17] For this system, some relevant attempts have been made in the past in combining ab initio and experimental information,[29,30] but they have been insufficient to adequately represent the long and intermediate range of the interaction.[15,17] Also, for the Cl + H_2 system, the importance of shallow wells located at intermediate intermolecular distance in the reactant and product valleys has been recently pointed out.[44]

The investigation and the application of a suitable representation for the asymptotic and intermediate behavior of the

† Part of the special issue "Aron Kuppermann Festschrift".

10.1021/jp003782r CCC: $20.00
Published on Web 02/24/2001

interaction in halogen atom − hydrogen molecule systems is one of the aims of this work. A spherical harmonic expansion is particularly convenient for this purpose: while the first term provides the isotropic component, higher order terms are required to account for the role of molecular anisotropy and atomic electronic orbital alignment. A special effort has been made to establish the nature of each radial coefficient of the expansion in order to assess its strength and its explicit dependence on the intermolecular distance.

The interaction potential expansion and the representation of the potential energy surfaces developed in this paper are an extension—including the role of fine structure effects and of nonadiabatic couplings—of the theory previously presented to describe bending levels in the P atom−linear molecule complexes.[45−48] For use of these potentials for reactive scattering calculations, see for example Ref 49. This work is also a generalization of the approach based on alternative angular momentum coupling schemes for the quantum mechanical treatment of collisions between atoms carrying spin and electronic angular momentum,[50,51] to take into account the effect of molecular orientation.

Formulas given in the following have been derived considering the ^{2}P character of the halogen atom and the nearly spherical shape of the H_2 molecule, considered as a rigid molecule frozen to the equilibrium distance. The method is currently being extended to other relevant cases, such as ^{2}P atom−homonuclear diatom more anisotropic than H_2, ^{2}P atom−heteronuclear diatom, ^{3}P or ^{1} D atom−diatomic molecule and also to systems including atomic and molecular ions. The proposed potential expansions provide the features of the potential energy surfaces for the F(^2P_j)-H_2 and Cl(^2P_j)-H_2 systems, which are relevant for collision dynamics calculations of elastic and inelastic processes occurring in the entrance channel of chemical reactions.

The present approach, which generates simultaneously both the ground and the lowest excited potential energy surfaces, provides a starting point to obtain the interaction in wider distance and orientation ranges, including possible molecular rearrangements leading to chemical reaction. For such developments, which involve the inclusion of the dependence of the bond stretching of the diatom, see Ref 52.

The paper is organized as follows: In Section II, the interaction potential expansion is presented, and the physical meaning of each radial term and its relation with the specific components of the interaction is discussed. Diabatic and adiabatic representations of the potential energy surfaces and the treatment of the nonadiabatic couplings are reported in Section III. In Section IV, the obtained results are shown, together with some comparisons between our results and the most recent and accurate ab initio potential energy surfaces. Discussion and conclusions follow in section V.

II. Harmonic Expansion: Role and Nature of the Radial Coefficients

A. Expansion. We develop our treatment with reference to a body-fixed frame where the quantization axis lies along the Jacobi vector $\vec{R}$, joining the atom to the center-of-mass of the molecule. The molecular axis $\vec{r}$ is oriented as $\hat{r} = (\theta, \phi)$ and the orientation of the half-filled orbital of the open-shell atom is given by $\hat{r}_e = (\theta_e, \phi_e)$. As can be seen from Figure 1, the problem is similar to the rotor−rotor model often employed for describing collisions of diatomic molecules. The formulation can also be presented exploiting such a similarity. Accordingly, the potential is expanded in a series of bipolar spherical harmonics, representing the angular dependence, and radial coefficients, which will be related to specific components of the atom−molecule interaction

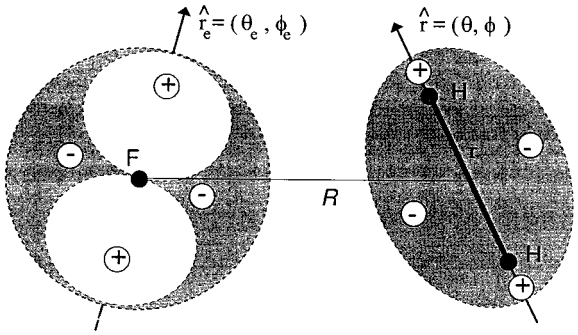

Figure 1. Illustration of a P-state atom−diatomic molecule interaction exploiting analogy with rotor−rotor case. Signs of quadrupolar moments are also indicated. The picture applies to the halogen atom−hydrogen molecule interaction.

$$V(R,r,\hat{r},\hat{r}_e) = \sum_{l_1,l_2,l_{12}} V^{l_{12}}_{l_1 l_2}(R,r)\, y^{l_{12}0}_{l_1 l_2}(\hat{r},\hat{r}_e) \qquad (1)$$

Here, the bipolar harmonics $y^{l_{12}0}_{l_1 l_2}$ are a linear combination of normalized spherical harmonics

$$y^{l_{12}0}_{l_1 l_2}(\hat{r},\hat{r}_e) = \sum_{\mu} \langle l_1 l_2 \mu - \mu | l_{12} 0\rangle\, Y_{l_1 \mu}(\hat{r}) Y_{l_2 -\mu}(\hat{r}_e) \qquad (2)$$

where $\langle ...|..\rangle$ is a Clebsch−Gordan coupling coefficient. In (2), l_1 and l_2 are angular momentum-like quantum numbers, l_{12} is their sum, and μ runs as their projection along the intermolecular axis $\vec{R}$. Ranges for the integers l_1 and l_2 will be related to the physically relevant molecular rotational and electronic orbital atomic states and will have to be restricted according to symmetries of the system.

The coefficients in expansion (1) are parametrical in R and r. In the following, we illustrate the case in which the molecular internuclear distance r is frozen at the equilibrium value (0.74 Å for H_2), so that any specific dependence on r will be omitted in the following. Such dependence has to be explicitly taken into account to describe reactions and vibrational excitations (negligible for H_2 collisions at thermal energies). For homonuclear molecules, only even l_1 values are permitted by the potential symmetry, while both even and odd terms are necessary to describe the case of heteronuclear diatoms. The number of terms requested by the expansion convergence depends on molecular anisotropy. For H_2, an expansion with $l_1 = 0, 2$ will be adopted to represent the molecular anisotropy.[53,54] As for l_1, the expansion for a P-state atom, such as F and Cl, will include $l_2 = 0, 2$, ($l_2 = 4$ is needed for a D atom,...[50]). This is sufficient to describe fine-structure, as long as configuration interactions to higher states is small. The potential must be invariant under the inversion of all the coordinates, and this symmetry limits the expansion in (1) to even values of $l_1 + l_2 + l_{12}$. As a consequence, l_{12}, corresponding to the coupling of the first two, is also even.

B. Radial Coefficients. An important target of the present analysis is to find a proper correspondence among the radial coefficient $V^{l_{12}}_{l_1 l_2}(R)$, introduced in eq 1, and the various components of the interaction, arising from dispersion, induction, electrostatic, charge-exchange effects, and also with repulsion, due to atomic and molecular sizes. Such a correspondence permits to obtain, for the prototype F(^2P_j)-H_2 and Cl(^2P_j)-H_2

systems, these crucial quantities from experimental information or from correlation formulas, which provide the main features of each interaction component in terms of fundamental physical properties of the interacting partners. In the following, a brief discussion about the role and the nature of each radial coefficient in open-shell atom−homonuclear diatom system is presented. Their explicit parametric form for the $F-H_2$ and $Cl-H_2$ cases is given in the Appendix.

The V_{00}^0 coefficient describes the spherical component of the interaction: it corresponds to that which is left after averaging on the relative orientation of the half-filled orbital of the open-shell atom and of the molecular axis. The V_{20}^2 term defines the change in the interaction due to different orientation of the molecule, taking the partner as a spherical atom, whereas the V_{02}^2 coefficient is related to the anisotropy due to the different possible orientations of the open-shell atom, the molecular partner being this time considered as a spherical particle. The other terms V_{22}^0, V_{22}^2, and V_{22}^4 emphasize the role of anisotropy effects arising from different relative positions of the open-shell atom with respect to the molecule: it is sufficient to average over the permitted orientations of a single partner to vanish their role.

Integral cross section measurements carried out for both $F(^2P_j)$-D_2[8] and $Cl(^2P_j)$-D_2 systems,[10] maintaining the target hydrogen molecule at sufficient high rotational temperature and using state-selected halogen beams, have provided direct information on the spherical components (V_{00}^0) and on the anisotropy associated with atomic orbital alignment effects (V_{02}^0).

The main features found[8,10] for the spherical component of the interaction, such as the depth and the position of the potential well, agree with the predictions based on empirical formulas,[55,56] which establish a correlation with the mean polarizability of the interacting partners. The agreement, also found for many other cases, suggests for such a term a typical van der Waals nature, being irrelevant contributions such as those due to electronic angular momentum couplings and charge exchange. (A method for the evaluation of these terms, also extended to include the case of atomic and molecular ions, has been given in Refs 55 and 56.) Accordingly, as reported in the Appendix, we adopted for V_{00}^0 (R) a standard parametrization for van der Waals forces and used the experimentally determined parameters.

In systems involving open-shell atoms or ions with high electron affinity, as the present ones, the V_{02}^2 component, associated with the alignment effects of the half-filled orbital of the open-shell atom, is mainly determined by charge-exchange effects, whereas van der Waals anisotropic contributions are less important except at large intermolecular distances. Charge-exchange effects basically depend on the overlap integral between orbitals describing the electron before and after the jump and on the energy splitting between involved states.[57] Their importance increases when the intermolecular distance, R, decreases and crucial is the role of the orientation of the atomic half-filled orbital. In the present cases, the R dependence of the V_{02}^2 term has been modeled as in Refs 8 and 10 by the combination of a decreasing exponential, accounting for the variation of the overlap integral, with an R^{-6} term, associated with the contribution of van der Waals nature arising from the halogen polarizability anisotropy. Also for the V_{02}^2 coefficient we have used the experimentally determined parameters. More details are given in the Appendix.

To put this approach in a proper perspective, we note that recently particular attention has been devoted in our laboratory to the characterization of the charge-transfer role in the bond stabilization in systems involving halogen, oxygen and sulfur atoms, and in symmetric and asymmetric rare gas ionic dimers,[58] at the crossings between ionic and covalent states[59] and in the proton affinity.[60] This study has led to a general correlation formula, given in terms of polarizability of the involved partners, electron affinity of the electron acceptor and ionization potential of the donor, which interpolates the behavior observed in several cases and permits to predict strength and distance dependence of this component for a variety of systems.[60]

The V_{20}^2 radial coefficient describes the anisotropy due to the different orientations of the molecule in the complex. This term, of van der Waals nature, arises from the combination of a contribution due to the modifications in the molecular size dominating at short range, and of a component describing the variation of the attractive forces. This component prevails at large R and is expected to be mainly determined by the anisotropy of the molecular polarizability. The first term has been represented by an exponential function, whereas the second behaves as R^{-6}.[61] To define the parameters of V_{20}^2 for $F-H_2$ and $Cl-H_2$, we have used the criteria given in Refs 53 and 54, where the behavior of the analogous terms for the "similar" $Ne-H_2$ and $Ar-H_2$ systems, has been experimentally characterized with great detail. Such a "similarity" comes from the very close value of the isotropic component of the polarizability of F and Cl atoms (0.56 and 2.18 Å^3) with those of Ne and Ar (0.40 and 1.64 Å^3).[62]

Also for these components of the interaction, we note that a recent extension of correlation formulas for van der Waals forces allows to predict their anisotropic character, both in the attractive and the repulsive region, in terms of the anisotropy of the molecular polarizability.[63] When atomic ions are involved this term must include further effects, due to ion−molecule quadrupole interaction.[64]

The V_{22}^0 and V_{22}^2 coefficients must be thought as corrective terms to the previously analyzed V_{20}^2 and V_{02}^2. Their physical meaning is less definite because they account for the modulation of charge exchange effects and van der Waals forces by a simultaneous variation in the orientation of the P atom and the diatomic molecule. Being higher order terms, they are expected to be small. In the present work, we represent them as decreasing exponential functions estimated from the behavior of similar terms in diatom−diatom systems such as N_2-N_2[61] and O_2-O_2.[65]

A most important and specific role is played by the V_{22}^4 coefficient, which describes the electrostatic interaction between the permanent quadrupoles of the atom and of the molecule. This term, which varies as R^{-5}, can be evaluated accurately because the quadrupole moment of H_2 is known[66] and that of the halogen atom can be given in terms of the mean square radius of the valence electrons (see Appendix).[45] For the present systems, in the Σ electronic state, one expects a marked repulsive effect for a linear complex, and a strong attraction for the bent geometry. The effect is smaller and opposite in the Π electronic states. Such an interaction is expected to play a crucial role in the intermediate intermolecular distance range affecting rotational inelastic collisions at thermal energies.[11,15,17]

III. Potential Energy Surfaces

The potential expansion given in eq 1 allows us to factorize the relative role of the components of the interaction for open-

shell atom−diatomic molecule systems and to model them using experimental information and correlation formulas. Dynamical calculations require a proper representation of the potential energy surfaces characterizing the investigated system. To do this, a suitable electronic basis must be chosen to give, after integration over the electronic coordinates, a diabatic representation of the potential energy surfaces, including atomic fine structure effects. Some alternative possibilities will be explored below. Then, adiabatic states can be obtained by diagonalization of the potential matrix. Such representations of the surfaces as a function of the nuclear variables R and θ (all the electronic features having been included in them) will be presented and illustrated in view of their exploitation for dynamical calculations.

To this aim, let us introduce "mixed" coefficients $V_{l_2\mu}(R,\hat{r})$ (i.e., depending on both R and θ) in terms of which the interaction potential reads

$$V(R,\hat{r},\hat{r}_e) = \sum_{l_2\mu} V_{l_2\mu}(R,\hat{r})\, Y_{l_2-\mu}(\hat{r}_e) \tag{3}$$

These terms are obtained as an alternative coupling scheme from the radial coefficients $V_{l_1l_2}^{l_{12}}$ of eq 1

$$V_{l_2\mu}(R,\hat{r}) = \sum_{l_1l_{12}} \langle l_1 l_2 \mu - \mu | l_{12} 0\rangle\, V_{l_1l_2}^{l_{12}}(R)\, Y_{l_1\mu}(\hat{r}) \tag{4}$$

It should be noted that the form of the potential in eq 3 can be considered as a generalization of the expansion familiar for open-shell closed-shell atom − atom interactions (see Ref 50). Accordingly, the description of the systems must be completed by considering the fine structure of the open-shell atom, represented by a phenomenological operator

$$\hat{H}_{so} = -\frac{2}{3}\delta\, \hat{L}\cdot\hat{S} \tag{5}$$

where δ will be empirically taken as the spin−orbit splitting of the open-shell atom, specifically 50.1 meV for F and 109.4 meV for Cl. In (5), $\hat{L}$ and $\hat{S}$ are the electronic orbital and spin angular momentum operators, respectively.

A. Diabatic Representation. Here, we focus on the electronic basis functions of the halogen atom, which in the treatment carried out so far depend on angular coordinates which individuate the orientation of the half-filled orbital of the open-shell atom, and as well exhibit a dependence on the spin coordinate of the unpaired electron. Alternative representations are possible, the simplest option being an electronically diabatic basis $Y_{L\Lambda}(\theta_e,\phi_e)\, X_{S\Sigma}(\sigma)$, where σ is a spin coordinate. In the following, we will indicate the electronic functions by the Hund's case (a) notation $|\Lambda\Sigma\rangle$ (for a ^{2}P atom $\Lambda = 0, \pm 1$ and $\Sigma = \pm {}^1/_2$). Parity is not introduced explicitly: its effects will be seen later by the splitting of the basis set. This latter is an atomic uncoupled basis in which the spin−orbit operator has both diagonal and off-diagonal elements

$$\langle \Lambda\, \Sigma \,|\, \hat{L}\cdot\hat{S} \,|\, \Lambda\, \Sigma \rangle = \Lambda\, \Sigma$$

$$\langle \Lambda\, \Sigma \,|\, \hat{L}\cdot\hat{S} \,|\, \Lambda \pm 1\, \Sigma \mp 1 \rangle =$$

$$\frac{1}{2}\,[L(L+1) - \Lambda(\Lambda \pm 1)]^{1/2}\,[S(S+1) - \Sigma(\Sigma \mp 1)]^{1/2} \tag{6}$$

The potential matrix, whose elements can be indicated as $\langle\, \Lambda\, \Sigma \,|\, V + H_{so} |\, \Lambda'\, \Sigma' \rangle$, after the integration over all the electronic coordinates, is real and symmetric and can be cast in the following form

$$\mathbf{W} = \begin{pmatrix} \mathbf{A} & -\mathbf{B} \\ \mathbf{B} & \mathbf{A} \end{pmatrix} \tag{7}$$

where

$$\mathbf{A} = \begin{pmatrix} V_{00} + \frac{2}{5}V_{20} & 0 & \sqrt{2}/3\,\delta \\ 0 & V_{00} - \frac{1}{5}V_{20} - \delta/3 & -\frac{\sqrt{6}}{5}V_{22} \\ \sqrt{2}/3\,\delta & -\frac{\sqrt{6}}{5}V_{22} & V_{00} - \frac{1}{5}V_{20} - \delta/3 \end{pmatrix} \begin{matrix} |0^1/_2\rangle \\ |-1-^1/_2\rangle \\ |1-^1/_2\rangle \end{matrix} \tag{8}$$

and

$$\mathbf{B} = \begin{pmatrix} 0 & \frac{\sqrt{3}}{5}V_{21} & -\frac{\sqrt{3}}{5}V_{21} \\ -\frac{\sqrt{3}}{5}V_{21} & 0 & 0 \\ \frac{\sqrt{3}}{5}V_{21} & 0 & 0 \end{pmatrix} \begin{matrix} |0-^1/_2\rangle \\ |1^1/_2\rangle \\ |-1^1/_2\rangle \end{matrix} \tag{9}$$

The terms $V_{l_2\mu}(R,\hat{r})$ in the last two equations have been defined in eq 4. The structure of the potential matrix allow us to apply a unitary transformation which brings the matrix into a factorized form, with two 3×3 blocks. Such a transformation can be written in explicit form as

$$\mathbf{U} = \frac{1}{\sqrt{2}}\begin{pmatrix} \mathbf{1} & \mathbf{1} \\ -i\mathbf{1} & i\mathbf{1} \end{pmatrix} \tag{10}$$

where $\mathbf{1}$ is the 3×3 unit matrix. The application of $\mathbf{U}$ to the complete potential matrix, as already stressed, makes the original matrix a factorized one having the following structure

$$\mathbf{U}^\dagger\, \mathbf{W}\, \mathbf{U} = \begin{pmatrix} \mathbf{A} + i\mathbf{B} & 0 \\ 0 & \mathbf{A} - i\mathbf{B} \end{pmatrix} \equiv \begin{pmatrix} \mathbf{V} & 0 \\ 0 & \mathbf{V}^* \end{pmatrix} \tag{11}$$

Each of the two blocks of dimension 3×3 is Hermitian. They have real and coincident eigenvalues, so that it is sufficient to proceed taking into account only one of the blocks.

Because the spin−orbit operator is not diagonal in the uncoupled basis $|\, \Lambda\, \Sigma\, \rangle$, a transformation to a diagonal form can be made using Clebsch−Gordan coupling coefficients to obtain the Hund's (c) case coupled basis $|\, j\, \Omega\, \rangle$

$$|\, j\Omega\rangle = \sum_{\Lambda\Sigma} \langle LS\Lambda\Sigma \,|\, j\Omega\rangle \,|\, \Lambda\Sigma\rangle \tag{12}$$

Here, j is the total electronic angular momentum of the atom ($j = {}^3/_2$ and $j = {}^1/_2$) and Ω its projection on the intermolecular axis R of the chosen rotating frame (phases and parity are here ignored for simplicity, see e.g., Ref 50).

As a consequence of this transformation, the following diabatic representation of the potential energy matrix is obtained

$$V_{00}\,\mathbf{1}+\frac{1}{3}\begin{pmatrix}0 & -\frac{2\sqrt{3}}{5}V_{22} & -\frac{3\sqrt{2}}{5}V_{20}\\ -\frac{2\sqrt{3}}{5}V_{22} & -\frac{3}{5}V_{20} & -\frac{3\sqrt{2}}{5}V_{22}\\ -\frac{3\sqrt{2}}{5}V_{20} & -\frac{3\sqrt{2}}{5}V_{22} & \frac{3}{5}V_{20}\end{pmatrix}\pm$$
$$i\begin{pmatrix}0 & \frac{1}{5}V_{21} & -\frac{\sqrt{3}}{5}V_{21}\\ -\frac{1}{5}V_{21} & 0 & +\frac{\sqrt{2}}{5}V_{21}\\ \frac{\sqrt{3}}{5}V_{21} & -\frac{\sqrt{2}}{5}V_{21} & 0\end{pmatrix}+\delta\begin{pmatrix}\frac{2}{3} & 0 & 0\\ 0 & -\frac{1}{3} & 0\\ 0 & 0 & -\frac{1}{3}\end{pmatrix} \quad (13)$$

where the signs + and − gives **V** and **V***, respectively.

B. Adiabatic Representation. The diagonalization of the diabatic potential matrix provides the electronically adiabatic eigenstates, i.e., the expression of the potential energy surfaces for the investigated systems as a function of R and of the bending angle θ. This involves the solution of a secular cubic equation: the corresponding roots represent the electronic adiabatic states, directly comparable with the Born−Oppenheimer potential energy surfaces as obtained in an ab initio calculation. The obtained surfaces correlate asymptotically with the spin−orbit states ^2P_j ($j = {}^3/_2$ and ${}^1/_2$) of the halogen atom.

The opposite limit would be when fine structure effects can be neglected, and the intermolecular interaction dominates. In such a case, the potential matrix resulting by integration over the spatial electronic coordinates θ_e and ϕ_e can be factorized into two mono- and bidimensional submatrices corresponding to the A″ and A′ symmetries typical of a triatomic system

$$V_{00}\,\mathbf{1}+\frac{1}{5}\begin{pmatrix}2V_{20} & \sqrt{6}V_{21} & 0\\ \sqrt{6}V_{21} & -V_{20}+\sqrt{6}V_{22} & 0\\ 0 & 0 & -V_{20}-\sqrt{6}V_{22}\end{pmatrix}\begin{matrix}p_z\\ p_x\\ p_y\end{matrix} \quad (14)$$

This latter is the same matrix obtained by Dubernet and Hutson[45] using directly a spin-free atomic p-orbital basis. Eigenvalues in this representation can be explicitly obtained, and the electronic states correlate with the barycenter of the asymptotic state ^2P of the isolated atom.

It should be noted that the atomic p-orbital set is a diabatic basis. However, at the linear geometry, the terms V_{21} and V_{22} vanish because the correspondent spherical harmonics are zero, so that the potential matrix on the given basis is diagonal there. Such a configuration allows us to identify the electronic states with the label Λ corresponding to the projection along $\vec{R}$ of the total orbital angular momentum $\vec{L}$ (Σ and Π are the usual notation for $\Lambda = 0$ and ± 1, respectively)

$$V_\Sigma = V_{00}(R,0)+\frac{2}{5}V_{20}(R,0)$$
$$V_\Pi = V_{00}(R,0)-\frac{1}{5}V_{20}(R,0) \quad (15)$$

The matrix (14) is diagonal also in the other limiting case, i.e., for the T-shape configuration of the three atoms corresponding to $\theta = \pi/2$. In the limit of a perpendicular geometry, the potential curves can be labeled with the irreducible representations (A_1, B_1, B_2) of the C_{2v} symmetry group to which the triatomic complex belongs. For all the intermediate geometries between the collinear and the perpendicular limits, covered by the range of the possible θ values between 0 and $\pi/2$, the surfaces are identified by the symmetry representations of the C_s group, 1 A′, A″, and 2 A′, respectively. These latter, arising from the solution of the simple secular problem in eq 14, are the adiabatic potentials which are presented and illustrated in Section IV.

C. Nonadiabatic Couplings. In the adiabatic representation, nonadiabatic coupling terms arise. Providing a functional expression of such couplings, which play a significant role in the dynamics, will be the focus of this section.

The treatment will refer to the spin-free p-orbitals atomic basis, a choice which involves no loss of generality. Only the x and z components will be considered, the p_y orbital being uncoupled by symmetry. We have already stressed that the p-orbitals are a diabatic basis set (see eq 14), providing a nondiagonal representation of the potential matrix. To obtain the electronic adiabatic eigenstates of A′ symmetry, which will be denoted as ϕ_1 and ϕ_2, a two-dimensional orthogonal transformation on this set must be performed

$$\begin{pmatrix}\phi_1\\ \phi_2\end{pmatrix}=\begin{pmatrix}\cos\gamma & -\sin\gamma\\ \sin\gamma & \cos\gamma\end{pmatrix}\begin{pmatrix}p_x\\ p_z\end{pmatrix} \quad (16)$$

where γ is the mixing angle dependent on the internal coordinates R and θ for the upper block in eq 14

$$\gamma(R,\theta)=\frac{1}{2}\arctan\frac{2\sqrt{6}V_{21}}{-3V_{20}+\sqrt{6}V_{22}} \quad (17)$$

Here, nonadiabatic terms, due to the interaction between the two electronic states induced by the nuclear motion will be examined, the fine structure effects having been already taken into account (Section III.A). A functional expression is found for the quantities

$$P^R(R,\theta)\equiv\langle\phi_1|\frac{\partial}{\partial R}|\phi_2\rangle=\frac{\partial\gamma}{\partial R} \quad (18)$$

$$P^\theta(R,\theta)\equiv\frac{1}{R}\langle\phi_1|\frac{\partial}{\partial\theta}|\phi_2\rangle=\frac{1}{R}\frac{\partial\gamma}{\partial\theta} \quad (19)$$

Obviously, they will show a dependence on both coordinates, as one can deduce looking at the expression (17) of the mixing angle γ used for the transformation of the diabatic basis to an adiabatic one. The $1/R$ scaling of P^θ brings it into units suitable for comparison. In the next section, we will proceed showing some plots of these nonadiabatic couplings terms in order to give an insight of their trends.

IV. Results

The spherical harmonic expansion discussed in Section II, which makes use of the radial coefficients whose parameters are reported in the Appendix, and the representations of the interaction discussed in Section III, permit to generate the three lowest potential energy surfaces for F(^2P_j)-H_2 and Cl(^2P_j)-H_2 systems. In this section, a pictorial representation of the obtained results will be given, together with some comparison with recent ab initio surfaces.[32,34] We first refer to the p-orbital basis introduced in Section III to focus the attention on the principal components of the interaction, and then introduce the effects due to spin−orbit, presenting some cuts of the surfaces for both investigated systems as a function of one of the two nuclear variables R and θ, for fixed values of the other one.

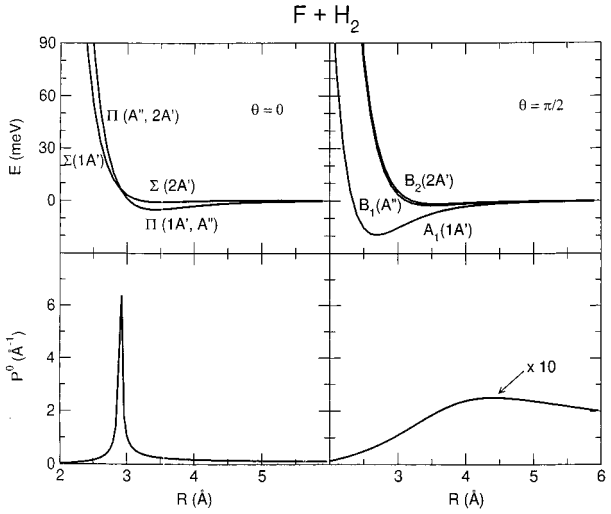

Figure 2. Relevant features of the interaction as a function of the internuclear distance R for the F−H_2 system. (Panel a): Adiabatic potential curves for the collinear configuration ($\theta = 0$) labeled in terms of the representations Σ and Π of $C_{\infty v}$ symmetry group. Corresponding states of C_s group are shown in parentheses. (Panel b): Adiabatic potential curves at the perpendicular configuration ($\theta = \pi/2$) labeled in terms of the representations of C_{2v} symmetry group. As in (Panel a), corresponding states of C_s group are shown in parentheses. (Panel c): Nonadiabatic coupling term P^θ between the A′ states for the collinear configuration. The corresponding term P^R is always zero for $\theta = 0$. (Panel d): Nonadiabatic coupling term P^θ between the A′ states for the perpendicular configuration. As it happens for $\theta = 0$, P^R vanishes everywhere.

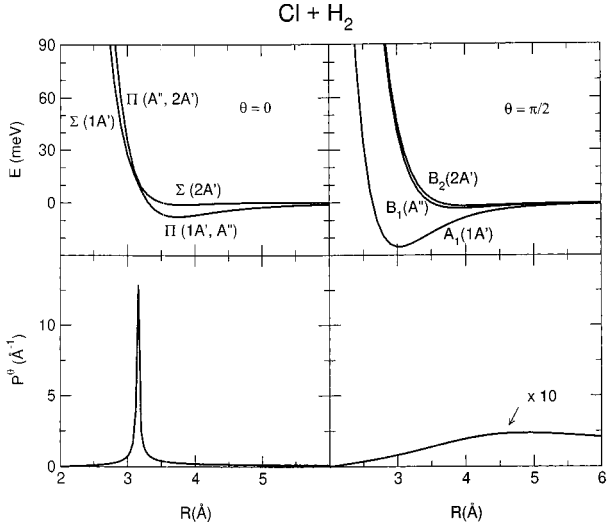

Figure 3. Relevant features of the interaction as a function of the intermolecular distance R for the Cl + H_2 system (see caption of Figure 2).

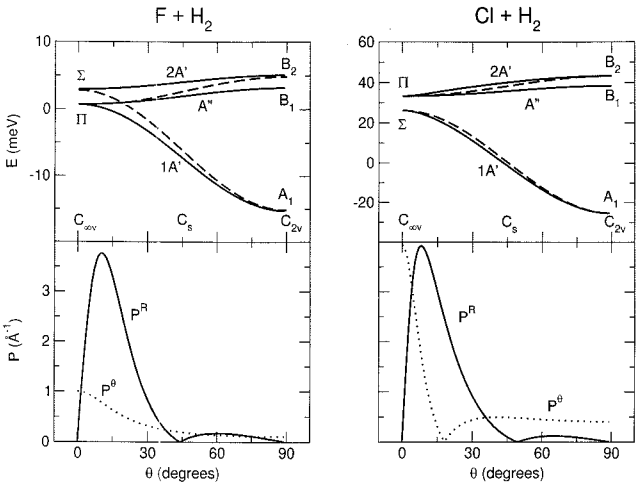

Figure 4. Relevant features of the interaction as a function of the θ orientational angle at fixed R for both investigated systems. Upper panels: Adiabatic potential curves (continuous curves) as a function of θ, at $R = 3.0$ Å. The correlation between symmetry representations in the two limit cases ($C_{\infty v}$ and C_{2v} correspond to the linear and perpendicular configurations, respectively) is shown. Also diabatic states (dashed lines) have been reported. Differences in the correlation diagrams are due to the fact that the chosen distance is larger than the avoided crossing for the F-system, but lower for the Cl-system. Lower panels: Non-adiabatic coupling terms P^θ (dotted curve) and P^R (continuous curve).

The adiabatic curves for the F(^2P_j)-H_2 system, in the two limiting nuclear configurations (corresponding to $\theta = 0$ and $\theta = \pi/2$), are plotted as a function of R in Figure 2.

In the $C_{\infty v}$ symmetry (collinear geometry), the diabatic electronic states can be labeled in terms of projections $\Lambda = 0$ (Σ), and ± 1 (Π) of the orbital electronic angular momentum $L = 1$ along the intermolecular axis R. The corresponding Σ and Π states cross at $R \approx 2.9$ Å, and the second one is energetically lower at long-range. The ground state exhibits a potential well with a minimum location at 3.4 Å and a depth of about 5 meV. Uncertainties are of the same magnitude as given in Ref 8. The observed sequence can be explained by invoking the quadrupole−quadrupole interaction between the atom and the molecule. It should be noted that the two Π curves coalesce as expected because of the same relative orientation of the half-filled orbital of the open-shell atom−molecule in the two cases. The adiabatic states are very close to those in the diabatic representation except for the effect of the avoided crossing.

In the C_{2v} symmetry (perpendicular geometry) the curves are labeled by the irreducible representations A_1, B_1, and B_2 of the symmetry group of the triatom. The ground state, corresponding to A_1 symmetry exhibits a well with a minimum at 2.7 Å and a depth of about 20 meV. Near fully repulsive curves correspond to B_1 and B_2 states; they are slightly split at all intermolecular distances because of differences in the relative orientation of the half-filled orbital of the halogen with respect to the molecule.

Figure 2 also includes the θ-coupling P^θ at $\theta = 0$ and $\pi/2$, the R-coupling P^R being everywhere zero for such limiting geometries. In the collinear geometry, Σ and Π states cross at R about 2.9 Å or, in the adiabatic picture, the two A′ states exhibit for such a distance an avoided crossing. Nonadiabatic couplings are actually peaked around $R \approx 2.9$ Å, and practically negligible elsewhere. As θ increases, the P^θ couplings monotonically decrease, the peak becomes smoother and smoother and moves toward larger R values, until the limit case shown in Figure 2 for $\theta = \pi/2$.

Figure 3 shows corresponding results for Cl−H_2 system. Minima of the wells are located at $R \approx 3.7$ Å and $R \approx 3.0$ Å for the collinear and perpendicular case, whereas depths are $\sim$ 8 and 25 meV, respectively. Again, uncertainties are of the same magnitude as given in Ref 10. Differences with respect to F−H_2 are expected to depend on the increased strength of both attractive and repulsive interaction. Concerning the avoided crossing at 3.2 Å and nonadiabatic couplings for this system, all the considerations made above for F−H_2 are also valid here.

The dependence of the interaction on the angular variable θ for the ground and excited potential energy surfaces for both systems is reported in Figure 4. The correlation between collinear and perpendicular geometries is shown for both the diabatic and adiabatic representations. The intermolecular

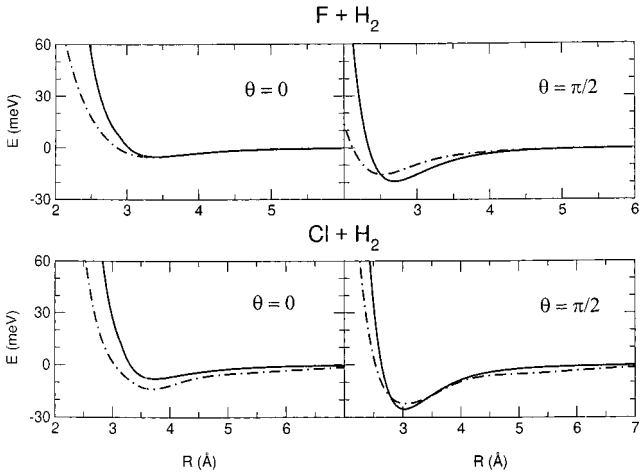

Figure 5. Comparison of present results for F−H_2 (upper panels) and Cl−H_2 (lower panels) in the ground adiabatic state 1A′ (solid curve) with those of Refs 32 and 34 (dashed−dotted line). Reported cuts as a function of R refer to the collinear ($\theta = 0$) and perpendicular ($\theta = \pi/2$) geometries.

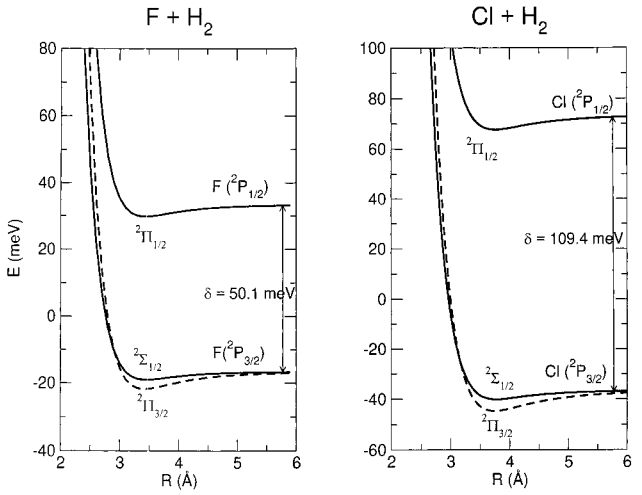

Figure 6. Adiabatic interactions including fine structure effects as a function of R for $\theta = 0$. Dashed line represents $^2\Pi_{3/2}$ curve, crossing the $^2\Sigma_{1/2}$ states at R around 2.9 Å for F−H_2 and 3.1 Å for Cl−H_2. The behavior of $^2\Pi_{1/2}$ state, correlating with the $^2P_{1/2}$ of the halogen atom is also shown. Asymptotic states are splitted by the atomic spin−orbit constant δ.

distance R has been fixed at 3.0 Å to allow a proper comparison with results of Ref 32 for F−H_2. This distance is larger than the avoided crossing distance for the F-system, but lower in the case of Cl, and this shows up as an apparent difference in the correlation diagrams. Nonadiabatic couplings P^R and P^θ are also plotted as a function of θ. Both terms seem to be more significant in the region around $\theta < 30°$. The P^θ couplings appear smaller as compared with the P^R terms except for $\theta = 0$ and $\pi/2$.

For the F−H_2 case, the present ground potential energy surface qualitatively agree with calculations of Stark and Werner.[32] Present data exhibit a larger anisotropy on θ angle, and some relevant differences in the R dependence. A quantitative comparison is shown in the upper panels of Figure 5. For the perpendicular approach, the present treatment provides an interaction energy more attractive at long distances but much more repulsive when R decreases. In the intermediate region, the balance of the two components of the interaction produces a deeper well localized at a larger distance. In the case of $\theta = 0$, the wells have similar depth but they look very different in the repulsive wall.

Also for the Cl + H_2 system, the well depth in the perpendicular configuration (see Figure 5, lower panels) is in reasonable agreement with a recent ab initio calculation (about 22 meV).[34] Dynamical calculations on the latter have demonstrated that the potential well found in the entrance channel plays a decisive role in the product distribution of the Cl + HD reaction.[44] Relevant differences between the two surfaces appear in the collinear geometry ($\theta = 0$).

Figure 6 shows, for the collinear configuration of the three atoms, the electronic adiabatic states for both systems arising from the diagonalization of one of the 3 by 3 blocks of the complete potential matrix, see eq 11. Reported curves represent the eigenvalues of (13) in the general case where both intermolecular potential and spin−orbit coupling are included. Curves in Figure 6 constitute then "true" adiabatic states,[67−69] as they have been obtained by the complete diagonalization of the general form of the interaction potential matrix, *i.e.* accounting also for the fine structure. As noticed in section III, such curves correlate asymptotically with the $|\, j\ \Omega\ \rangle$ spin−orbit states of the halogen atom and providing more insight than the results reported in Figures 2 and 3. In Figure 6, the $^2\Pi_{3/2}$ curve crosses the $^2\Sigma_{1/2}$ states at R around 2.9 Å for F−H_2 and at R around 3.2 Å for Cl−H_2. The remaining $^2\Pi_{3/2}$ state is the only one correlating with the $^2P_{1/2}$ of the halogen atom.

V. Discussion and Conclusions

In this paper, we have developed a general method to evaluate the intermolecular potential of a diatomic molecule with an open-shell atom in the configuration region where the collision dynamics is controlled by intermediate (a few Å) and long-range (tens of Å) anisotropic forces, essentially where potentials are negative. The potential is expressed as a harmonic expansion whose moments give the dependence of the interaction on the intermolecular distance. For F−H_2 and Cl−H_2 systems relevant contributions arise from the spherical component V^0_{00}, of van der Waals nature, from the anisotropic coefficients V^2_{02} and V^2_{20}, which describe effects due to atomic alignment and to molecular orientation, and from V^4_{22} component which defines the quadrupole−quadrupole interaction (the V^0_{22} and V^2_{22} coefficients represent minor contributions). The proper combination of experimental information with the predictions of correlation formulas provides strength and intermolecular distance dependence of these components. A simultaneous description of both ground and excited potential energy surfaces, as a function of intermolecular distance and bending angle, has been the outcome of our procedure and constitutes a platform for applications to molecular dynamics. These applications require further improvements on the approach presented here, which has concerned the introduction of spin−orbit effects and the evaluation of nonadiabatic couplings, allowing proper description of elastic and inelastic scattering. As for the opening of possible reactive paths, involving the inclusion of the dependence of the potential energy on the molecular bond length, see Ref 52.

The reported results emphasize that the H_2 orientational anisotropy is markedly different for the 1A′, 2A′, and A″ potential energy surfaces because of the different role of the components contributing to the global interaction. Therefore, the rotational inelasticity is expected to be strongly dependent on the symmetry properties of the involved potential energy surface. Pronounced wells are present near the perpendicular configuration: their depths (about 20 and 25 meV, respectively, for F−H_2 and Cl−H_2) agree with the predictions of ab initio

calculations,[32,34,44] whereas the location of the well for $F-H_2$ is significantly larger (see Section IV).

Depths and locations of such wells could affect the collision dynamics at least at thermal energies; this point has been recently addressed in a paper focused on the role of the entrance valley for the Cl + HD reaction.[44] However, detailed calculations of reactive dynamics require a complete description of the interaction in the whole configuration space of the three atoms. As previously discussed, our representation is appropriate for the intermediate and long intermolecular distances both in the entrance and exit channels, whereas it is inadequate in the strong interaction region where the triatomic complex undergoes a molecular rearrangement. A first attempt to carry out extensive dynamical calculations is founded on the merging of the potential energy surfaces determined in this paper with those obtained fitting ab initio data which simulate accurately the triatomic interaction in the transition state region; this matching is required for getting the reactive path open as the intermolecular distance becomes sufficiently small.

The merging of our ground surface with available ab initio potential energy surfaces (see 39 and 52, where the new PES of 32 has been employed) allows us to perform reactive scattering quantum mechanical calculations for the $F-H_2$ system. State-to-state integral and differential cross sections apex have been calculated and compared with those from analogous calculations carried out on the surface in Ref 32. Preliminary comparisons with Ref 38 indicate improvement on agreement with available experimental measurements,[6] notably for the production of the HF molecule in the final vibrational state $v' = 3$.

In conclusion, we note that the features of the proposed potentials, originating from a critical balancing between electrostatic, van der Waals and charge-transfer components, were extracted from total integral cross sections data, measured under high rotational temperature conditions,[8,10] for which orientational effects due to the H_2 molecule play a minor role. In particular, it can be checked that averaging over the possible H_2 orientations basically the electrostatic components vanishes and one obtains the potentials originally proposed in those papers,[8,10] which include only the van der Waals component and atomic alignment effects (essentially charge-transfer). In addition, in both cases, the anisotropy due to the H_2 orientation appears to be much larger than in the Ne and $Ar-H_2$ systems, on line with what appears to be required to describe inelastic differential cross section data.[11,15]

It would be desirable to reproduce all the properties available on such systems, including elastic, inelastic, and reactive cross sections, by using the same potential energy surfaces. Such an analysis should allow the determination of the relative role of elastic, inelastic and reactive collisions as a function of the angular momentum and of collision energy, providing also additional information to probe fine details of the potential energy surface in the transition state region.

Appendix: Parametrization of the Radial Coefficients

The $V_{00}^0(R)$ term—which describes spherical interaction of van der Waals nature (see text)—has been represented by the usual MSV (Morse- Spline-van der Waals) parametrization.[8,10] Two boundary points R_1 and R_2 are chosen, and a Morse function is used for R values smaller than R_1

$$V_{00}^0(R) = \epsilon\left\{\exp\left[-2\beta_m\left(\frac{R}{R_m}-1\right)\right] - 2\exp\left[-\beta_m\left(\frac{R}{R_m}-1\right)\right]\right\}$$

whereas a van der Waals dependence is employed for R values larger than R_2

$$V_{00}^0(R) = -C_{00}^0\, R^{-6}$$

The parameters ϵ and R_m represent the depth and the position of the minimum, whereas β_m is related to the curvature of the potential well, which is described by the Morse function. The C_{00}^0 term defines the long-range behavior of the potential, and controls the attractive part of interaction. A cubic spline function

$$f(R) = b_1 + \left(\frac{R}{R_m}-\frac{R}{R_1}\right)\left\{b_2 + \left(\frac{R}{R_m}-\frac{R}{R_2}\right)\left[b_3 + \left(\frac{R}{R_m}-\frac{R}{R_1}\right) b_4\right]\right\} \quad (20)$$

with coefficients b_i which ensure the continuity of the potential and of the first derivatives at the match points R_1 and R_2, covers the range between R_1 and R_2.

For the V_{02}^2 term, which represents the interaction anisotropy associated with the alignment of the open-shell atom, we have adopted the functional form

$$V_{02}^2(R) = -A_{02}^2\exp(-\alpha_{02}^2\times R) + C_{02}^2\, R^{-6}$$

where the exponential decay describes the variation of overlap effects of the half-filled orbital, dominant at short range, and the second term corresponds to the anisotropy of the long-range attraction.

All the parameters of V_{00}^0 and V_{02}^2, given in Tables 1 and 2, have been obtained from the analysis of scattering cross section data[8,10] (see text).

The following parametrization has been chosen for the V_{20}^2 term, which describes the effect of molecular anisotropy on a spherical atom

$$V_{20}^2(R) = A_{20}^2\times\exp\{-\alpha_{20}^2 R\} - C_{20}^2\, R^{-6}$$

where the exponential term has been fixed on the basis of the experimental results obtained for the systems H_2-Ar (in the case of the chlorine) e H_2-Ne (in the case of the fluorine).[53,54] The parameter C_{20}^2 can be expressed as a function of the

TABLE 1: Parameters for the $V_{00}^0(R)$ Radial Coefficients

coefficient		$F-H_2$	$Cl-H_2$
V_{00}^0	R_m (Å)	3.34	3.70
	ϵ (meV)	4.12	5.70
	β_m	6.30	6.30
	C_{00}^0 (meV Å^6)	7.52×10^3	2.60×10^4
	R_1	3.71	4.07
	R_2	5.01	5.92
	b_1	−0.7501	−0.7815
	b_2	1.6275	1.3511
	b_3	−3.9039	−3.5710
	b_4	2.3440	3.3269

TABLE 2: Parameters for the $V_{02}^2(R)$, $V_{20}^2(R)$ and $V_{22}^4(R)$ Radial Coefficients

coefficient		$F-H_2$	$Cl-H_2$
V_{02}^2	A_{02}^2(meV)	8.11×10^5	7.00×10^5
	α_{02}^2 (Å^{-1})	3.50	3.00
	V_{02}^2(meV Å^6)	9.02×10^2	4.70×10^3
V_{20}^2	A_{20}^2(meV)	1.30×10^5	4.26×10^5
	α_{20}^2 (Å^{-1})	3.50	3.50
	C_{20}^2(meV Å^6)	7.00×10^2	2.40×10^3
V_{22}^4	C_{22}^4(meV Å^5)	854	2245

polarizability anisotropy of molecular hydrogen.[67,70] The employed parameters are given in Table 2.

Following suggestions given in Refs 65 and 61, parameters for the V_{22}^0 and V_{22}^2 coefficients, which correspond to correction terms, have been assumed to be the same as those defining the exponential part of the term $V_{20}^2(R)$

$$\alpha_{22}^2 = \alpha_{22}^0 = \alpha_{20}^2$$

$$A_{22}^2 = -A_{22}^0 = -A_{20}^2$$

The quadrupole−quadrupole interaction term V_{22}^4 takes the known analytical expression

$$V_{22}^2(R) = k\, Q_1 Q_2 R^{-5} = C_{22}^4\, R^{-5}$$

where Q_1 and Q_2 represent the quadrupole momentum of the open-shell atom and of the diatomic molecule, respectively, and k is a normalization constant depending on the adopted spherical harmonic expansion. For an atom with electronic configuration p^5, the quadrupole moment can be evaluated as $e\,\langle r_a^2\rangle$,[45] where e is the electron charge and r_a is the mean square radius of the outer orbitals. The data are reported in Table 2.

Acknowledgment. It is a pleasure to dedicate to Professor Aron Kuppermann this paper on a theme—accurate potential energy surfaces for benchmark quantum reactive scattering calculations—for which he has been a pioneer. This work is supported by the Italian National Research Council (CNR), the Ministero dell'Università e della Ricerca Scientifica e Tecnologica (MURST), the European Union within the Human Potential Research Network "Theoretical Studies of Electronic and Dynamical Processes in Molecules and Clusters" (Contract No. HPRN-CT-1999-00005), the COST D9 Action, ENEA and INTAS.

References and Notes

(1) Casavecchia, P.; Balucani, N.; Volpi, G. G. *Annu. Rev. Phys. Chem.* **1999**, *50*, 347.
(2) Balakrishnan, N.; Dalgarno, A.; Forrey, R. C. *J. Chem. Phys.* **2000**, *113*, 621.
(3) Anderson, J. B. *J. Chem. Phys.* **1970**, *52*, 3849.
(4) Kumaram, S. S.; Lim, K. P.; Michael, J. V. *J. Chem. Phys.* **1994**, *101*, 9487.
(5) Taatjes, C. A. *Chem. Phys. Lett.* **1999**, *306*, 33.
(6) Neumark, D. M.; Wodtke, A. M.; Robinson, G. N.; Hayden, C. C.; Lee, Y. T. *J. Chem. Phys.* **1985**, *82*, 3045.
(7) Neumark, D. M.; Wodke, A. M.; Robinson, G. N.; Hayden, C. C.; Shobatake, R.; Sparks, R. K.; Schafer, T. P.; Lee, Y. T. *J. Chem. Phys.* **1985**, *82*, 3067.
(8) Aquilanti, V.; Candori, R.; Cappelletti, D.; Luzzatti, E.; Pirani, F. *Chem. Phys.* **1990**, *145*, 293.
(9) Faubel, M.; Schlemmer, S.; Sondermann, F.; Toennies, J. P. *J. Chem. Phys.* **1991**, *94*, 4676.
(10) Cappelletti, D.; Aquilanti, V.; Pirani, F. *J. Chem. Soc., Faraday Trans.* **1993**, *89*, 1467.
(11) Faubel, M.; Rusin, L. Y.; Schlemmer, S.; Sondermann, F.; Tappe, U.; Toennies, J. P. *J. Chem. Soc., Faraday Trans.* **1993**, *89*, 1475.
(12) Faubel, M.; Rusin, L. Y.; Schlemmer, S.; Sondermann, F.; Tappe, U.; Toennies, J. P. *J. Chem. Phys.* **1994**, *101*, 2106.
(13) Faubel, M.; Martínez-Haya, B.; Rusin, L. Y.; Tappe, U.; Toennies, J. P. *Z. Physik. Chemie* **1995**, *188*, 197.
(14) Alagia, M.; Balucani, N.; Cartechini, L.; Casavecchia, P.; van Kleef, E. H.; Volpi, G. G.; Aoiz, F. J.; Bañares, L.; Schwenke, D. W.; Allison, T. C.; Mielke, S. L.; Truhlar, D. G. *Science* **1996**, *273*, 1519.
(15) Gianturco, F. A.; Ragnetti, F.; Faubel, M.; Martínez-Haya, B.; Rusin, L. Y.; Sondermann, F.; Tappe, U. *Chem. Phys.* **1995**, *200*, 405.
(16) Chapman, W. B.; Blackmon, B. W.; Nesbitt, D. J. *J. Chem. Phys.* **1997**, *107*, 8193.
(17) Ayabakan, M.; Faubel, M.; Martínez-Haya, B.; Rusin, L. Y.; Sevryuk, M. B.; Tappe, U.; Toennies, J. P. *Chem. Phys.* **1998**, *229*, 21.
(18) Lee, S. H.; Liu, K. *J. Chem. Phys.* **1999**, *111*, 6253.
(19) Weaver, A.; Neumark, D. M. *Faraday Discuss. Chem. Soc.* **1991**, *91*, 5.
(20) Metz, R. B.; Bradforth, S. E.; Neumark, D. M. *Adv. Chem. Phys.* **1992**, *81*, 1.
(21) Neumark, D. M. *Annu. Rev. Phys. Chem.* **1992**, *43*, 153.
(22) Neumark, D. M. *Acc. Chem. Res.* **1993**, *26*, 33.
(23) Bradforth, S. E.; Arnold, D. W.; Neumark, D. M.; Manolopoulos, D. E. *J. Chem. Phys.* **1993**, *99*, 6345.
(24) Frisch, M. J.; Binkley, J. S.; Schaefer, H. F., III. *J. Chem. Phys.* **1984**, *81*, 1882.
(25) Steckler, R.; Schwenke, D. W.; Brown, F. B.; Truhlar, D. G. *Chem. Phys. Lett.* **1985**, *121*, 475.
(26) Schwenke, D. W.; Stekler, R.; Brown, F. B.; Truhlar, D. G. *J. Chem. Phys.* **1986**, *84*, 5706.
(27) Schwenke, D. W.; Stekler, R.; Brown, F. B.; Truhlar, D. G. *J. Chem. Phys.* **1987**, *86*, 2443.
(28) Takayanagi, T.; Sato, S. *Chem. Phys. Lett.* **1988**, *144*, 191.
(29) Lynch, G. C.; Stekler, R.; Schwenke, D. W.; Varandas, A. J. C.; Truhlar, D. G.; Garret, B. C. *J. Chem. Phys.* **1991**, *94*, 7136.
(30) Mielke, S. L.; Lynch, G. C.; Truhlar, D. G.; Schwenke, D. W. *Chem. Phys. Lett.* **1993**, *213*, 10.
(31) Mielke, S. L.; Lynch, G. C.; Truhlar, D. G.; Schwenke, D. W. *Chem. Phys. Lett. 217*, 173, 1994, erratum.
(32) Stark, K.; Werner, H.-J. *J. Chem. Phys.* **1996**, *104*, 6515.
(33) Allison, T. C.; Lync, G. C.; Trulhar, D. G.; Gordon, M. S. *J. Phys. Chem.* **1996**, *100*, 13 575.
(34) Bian, W.; Werner, H.-J. *J. Chem. Phys.* **2000**, *112*, 220.
(35) Launay, J. M.; Le Dourneuf, M. *Chem. Phys. Lett.* **1989**, *163*, 178.
(36) Baer, M.; Faubel, M.; Martínez-Haya, B.; Rusin, L. Y.; Tappe, U.; Toennies, J. P.; Stark, K.; Werner, H.-J. *J. Chem. Phys.* **1996**, *104*, 2743.
(37) Manolopoulos, D. E. *J. Chem. Soc., Faraday Trans.* **1997**, *93*, 673.
(38) Castillo, J. F.; Manolopoulos, D. E.; Stark, K.; Werner, H.-J. *J. Chem. Phys.* **1996**, *104*, 6531.
(39) Aquilanti, V.; Cavalli, S.; De Fazio, D.; Volpi, A.; Aguilar, A.; Gimenez, X.; Lucas, J. M. *J. Chem. Phys.* **1998**, *109*, 3805.
(40) Mielke, S. L.; Allison, T. C.; Truhlar, D. G.; Schwenke, D. W. *J. Phys. Chem.* **1996**, *100*, 13 588.
(41) Wang, H.; Thompson, W. H.; Miller, W. H. *J. Chem. Phys.* **1997**, *107*, 7194.
(42) Castillo, J. F.; Aoiz, F. J.; Bañares, L.; Martínez-Haya, B.; Hartke, B.; Werner, H.-J. *J. Chem. Phys.* **1998**, *109*, 7224.
(43) Alexander, M. H.; Manolopoulos, D. E.; Werner, H.-J. *J. Chem. Phys.* **1998**, *109*, 5710; *J. Chem. Phys.* **2000**, *113*, 11 084.
(44) Skouteris, D.; Manolopoulos, D. E.; Bian, W.; Werner, H.-J.; Lai, L.-H.; Liu, K. *Science* **1999**, *286*, 1713.
(45) Dubernet, M. L.; Hutson, J. M. *J. Chem. Phys.* **1994**, *101*, 1939.
(46) Dubernet, M. L.; Hutson, J. M. *J. Phys. Chem.* **1994**, *98*, 5844.
(47) Meuwly, M.; Hutson, J. M. *J. Chem. Phys.* **2000**, *112*, 592.
(48) Meuwly, M.; Hutson, J. M. *Phys. Chem. Chem. Phys.* **2000**, *2*, 441.
(49) Maierle, C. S.; Schatz, G. C.; Gordon, M. S.; McCabe, P.; Connor, J. N. L. *J. Chem. Soc., Faraday Trans.* **1997**, *93*, 709.
(50) Aquilanti, V.; Grossi, G. *J. Chem. Phys.* **1980**, *73*, 1165.
(51) Aquilanti, V.; Casavecchia, P.; Grossi, G.; Laganà, A. *J. Chem. Phys* **1980**, *73*, 1173.
(52) Volpi, A. *Tesi di Dottorato*, Università di Perugia, 2000.
(53) Andres, J.; Buck, U.; Huisken, F.; Schleusener, J.; Torello, F. *J. Chem. Phys.* **1980**, *73*, 5620.
(54) Buck, U. *Faraday Discuss. Chem. Soc.* **1982**, *73*, 187.
(55) Cambi, R.; Cappelletti, D.; Liuti, G.; Pirani, F. *J. Chem. Phys.* **1991**, *95*, 1852.
(56) Cappelletti, D.; Liuti, G.; Pirani, F. *Chem. Phys. Lett.* **1991**, *183*, 297.
(57) Krauss, M. *J. Chem. Phys.* **1977**, *64*, 1712.
(58) Aquilanti, V.; Cappelletti, D.; Pirani, F. *Chem. Phys. Lett.* **1997**, *271*, 216.
(59) Aquilanti, V.; Cappelletti, D.; Pirani, F. *J. Chem. Phys.* **1997**, *107*, 5043.
(60) Pirani, F.; Giulivi, A.; Cappelletti, D.; Aquilanti, V. *Mol. Phys.* **2000**, *98*, 1749.
(61) Cappelletti, D.; Vecchiocattivi, F.; Pirani, F.; Heck, E. L.; Dickinson, A. S. *Mol. Phys.* **1998**, *93*, 485.
(62) Miller, T. M.; Bederson, B. *Adv. At. Mol. Phys.* **1977**, *13*, 1.
(63) Cappelletti, D.; Pirani, F., work in progress.
(64) Buckingham, A. D. *Adv. Chem. Phys.* **1967**, *12*, 107.
(65) Aquilanti, V.; Ascenzi, D.; Bartolomei, M.; Cappelletti, D.; Cavalli, S.; de Castro Vítores, M.; Pirani, F. *J. Am. Chem. Soc.* **1999**, *121*, 10 794.
(66) Stogryn, D. E.; Stogryn, A. P. *Mol. Phys.* **1966**, *11*, 371.
(67) Tully, J. C. *J. Chem. Phys.* **1973**, *59*, 5122.
(68) Jaffe, R. L.; Morokuma, K.; George, T. F. *J. Chem. Phys.* **1975**, *63*, 3417.
(69) Lepetit, B.; Launay, J. M.; Le Dourneuf, M. *Chem. Phys.* **1986**, *106*, 111.
(70) Hirschfelder, J. O.; Curtis, C. F.; Bird, R. B. *The Molecular Theory of Gases and Liquids*; Wiley: New York, 1954.